

## Theoretical and experimental analysis of RHS/CHS K gap joints

### *Análise teórico e experimental de ligações tipo RHS/CHS com afastamento*

#### **Iara Souto Mayor**

Departamento de Engenharia Civil,  
Escola de Minas,  
Universidade Federal de Ouro Preto,  
Universidade Estadual de Campinas – UNICAMP.  
iaramapa@yahoo.com.br

#### **Gabriel Vieira Nunes**

Departamento de Engenharia Civil,  
Escola de Minas,  
Universidade Federal de Ouro Preto.  
gvnunes@yahoo.com.br

#### **Arlene M. S. Freitas**

Departamento de Engenharia Civil,  
Escola de Minas,  
Universidade Federal de Ouro Preto,  
arlene.freitas@gmail.com,  
arlene@em.ufop.br

#### **João A. V. Requena**

Universidade Estadual de Campinas – UNICAMP  
requena@fec.unicamp.br

#### **Afonso H. Araújo**

Vallourec Mannesmann do Brasil,  
Belo Horizonte, MG, Brasil  
afonso@vmtubes.com.br

#### **Resumo**

Nesse trabalho, é apresentado um estudo de ligações soldadas tipo K com afastamento, constituídas de barras tubulares de aço sem costura, sendo usada seção transversal tubular retangular, no banzo, e circular, para os outros elementos. O estudo envolveu análise teórica e numérica, para as ligações, além de ensaios de protótipos, em escala real. As análises teóricas utilizaram normas de projeto, para a ligação K. Os ensaios foram realizados, em protótipos, em escala real, visando à obtenção do comportamento, da carga última e do modo de falha da ligação e à calibração com modelo numérico (elementos finitos), bem como visando a se fazer uma comparação com prescrições normativas. Essas ligações ensaiadas apresentaram, como modo de falha, a plastificação da face do banzo (modo A). Os resultados numéricos indicaram que a relação entre as cargas numéricas e as de projeto, obtidas pelas prescrições, apresenta boa correlação, para ligações K.

**Palavras-chave:** Estruturas metálicas, estruturas tubulares, ligações.

#### **Abstract**

*This work presents a study of welded K joints with gap, formed by a structural steel hot rolled hollow section, having rectangular hollow sections at the chords and circular hollow sections in the others members. The study developed theoretical and numerical analyses for the joints, experimental tests in full scale prototypes. Theoretical analyses were performed using code standards for K joints. The results in terms of behavior, ultimate load and collapse mode were analyzed and compared with numerical (finite elements) and theoretical models. The theoretical analysis was carried out from the code regulations. The joints tested indicated the failure mode of Plastic failure of the chord face (mode A). The results showed that the loads using code regulations and the ones from the numerical analysis had good agreement for the K joint.*

**Keywords:** Steel structures, tubular structures, joints.

### 1. Introduction

Hollow structural sections (HSS) are being used more and more often in building construction and can be used efficiently in various structural systems, as truss systems. Different connections can be used in truss structural systems and depend on various factors, such as: architectonics, manufacturing, gap size, span and others.

The tubular steel profiles used in truss systems can be RHS (rectangular hollow sections), CHS (circular hollow

section), or a combination of CHS and RHS. For the cases of welded trusses, the joints can be T, K, and KT, for example.

The welded tubular K joint (Figure 1) with a gap,  $g$ , the eccentricity,  $e$ , can be classified as positive, null or negative. It is positive when the intersection of the brace axes is below the chord axis; on the other hand, negative eccentricity occurs when this point is above the chord axis and neutral when it is above the axis.

The welded tubular K joint with

RHS chord section and CHS braces present different failure modes. Table 1 presents a description of the failure modes within the specifications of K joints.

This paper reviews some design guidance on axial loaded resistance gap K-joints and an experimental program and numerical study of the strength is presented. The finite element model was calibrated with experimental results and the study of failure mode A was the focus. The numerical study was compared with design codes.

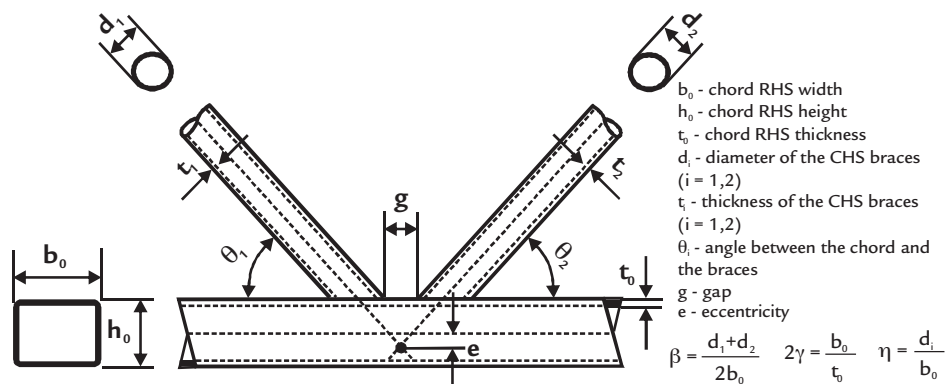


Figure 1  
The geometric parameters for K joints with gap.

Failure Mode	Failure Mode Description
A	Chord face failure (plastic failure of the chord face)
C	Chord side wall failure (or chord web failure ) by yielding, crushing or instability
D	Punching shear failure of a hollow section chord wall
E	Local buckling failure of a brace member

Table 1  
Failure modes for K tubular joints.

### 2. Design codes

This study used the Eurocode 3 - part 1.8 (Eurocode, 2005) standards for building, the Brazilian code (PN, 2011) and CIDECT formulation (Comité international pour le développement et l'étude de la construction tubulaire) (Wardenier

et al, 2010). The Eurocode and Brazilian code have the same equations for K joint axial force resistance.

The K joint design resistance should be taken as the minimum axial force value of the braces, calculated according to all

criteria of the failure modes, within the limits in Table 2.

The axial force resistance to chord face failure (mode A) for K joints should be determined according to the equations presented in Table 3.

### 3. Experimental program

Tests were performed for welded gap K joints by HHS (hot hollow section) tubular elements, where CHS was used for the braces and RHS for the chord. A total of three tests were performed. Table 4 presents the nominal dimensions of the RHS and CHS of the tested welded K joints. The prototype nomenclatures are K01, K02 and K03. Table 5 shows steel mechanical proprieties that were obtained by mechanical testing. (Mayor, 2010).

The experimental scheme design for the tests was developed by Mendanha et al. (2007) using accessory parts and fixed elements at the ends of the chord,

together with support elements for the hydraulic jack compression and tension application. These elements were designed to support the magnitude of the applied loads. Figure 2 shows the general layout of the tested joints.

To apply the tension load, a pin system was used to guarantee that there would be no load eccentricity and to maintain its application in the axis direction. For the compressed brace, a spherical plain connector was used to guarantee load verticality and to eliminate spurious moments.

The deformations and linear displacements were monitored during the

test. Linear Variable Displacement Transducers (LVDT) were used to obtain the linear displacements [Figure 3(A)]. Unidirectional strain gages (brace), and 45° rosettes [Figure 3(B)] were used to measure deformation. The loads were applied to the braces and measured by load cells.

An automatically acquisition system and software controlled the tests. From the test results, it was possible to verify that the most common failure mode was plastic failure of the chord face (mode A); data was obtained at rosette 2, located on the chord's superior surface between the braces.

		Valid conditions for K welded joints	
		PN and Eurocode	CIDECT
Eccentricity		$-0.55h_0 \leq e$ and $e \leq 0.25 h_0$	$-0.55h_0 \leq e$ and $e \leq 0.25 h_0$
Gap		$0.5 (1-\beta) \leq \frac{g}{b_0} \leq 1.5 (1-\beta)$ $g \geq t_1 + t_2$	$0.5 (1-\beta) \leq \frac{g}{b_0} \leq 1.5 (1-\beta)$ $\frac{g}{b_0} > t_1 + t_2$
Geometrical parameters	Rectangular	$0.5 \leq \frac{h_0}{b_0} \leq 2$ $\frac{b_0}{t_0} \leq 36$ $\frac{h_0}{t_0} \leq 36$	$\frac{b_0}{t_0} \leq 40$ and $\frac{h_0}{t_0} \leq 40$
	Circular	$\frac{d_i}{t_i} \leq 50$ $0.4 \leq \frac{d_i}{b_0} \leq 0.8$	$\frac{d_i}{t_i} \leq 40$
Slenderness limits	Rectangular	$\frac{b_0}{t_0} \leq 1.3 \sqrt{\frac{E}{f_y}}$ $\frac{h_0}{t_0} \leq 1.3 \sqrt{\frac{E}{f_y}}$	Class 1 33ε Class 2 38ε $\epsilon = \sqrt{\frac{235}{f_y}}$
	Circular	$\frac{d_i}{t_i} \leq 0.05 \frac{E}{f_y}$	Class 1 50ε Class 2 70ε $\epsilon = \sqrt{\frac{235}{f_y}}$

Table 2  
Valid conditions for the welded joints with CHS braces and RHS chord.

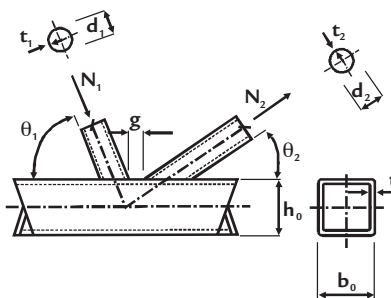
Failure mode A	PN and Eurocode	CIDECT
	$N_{1,Rd} = \frac{9.79 k_n f_y t_0 \sqrt{f_y}}{\sin(\theta_1)} \beta / \gamma_{a1}$ $N_{2,Rd} = \frac{\sin(\theta_1)}{\sin(\theta_2)} N_{1,Rd}$ <p>to <math>n &lt; 0</math> <math>k_n = 1.3 + \frac{0.4}{\beta}</math></p> <p>to <math>n \geq 0</math> <math>k_n = 1.0</math></p> $n = \frac{\sigma_{0,Sd}}{f_{y0}} \quad \sigma_{0,Sd} = \frac{N_{0,Sd}}{A} + \frac{M_{0,Sd}}{W_0}$ <p>compression is a negative sign.</p>	$N_i^* = Q_u Q_f f_{y0} t_0^2$ $Q_u = 14 \beta^{0.3}$ $Q_f = (1 -  n )^{C_1}$ <p>compression: <math>C_1 = 0.5-0.5n</math></p> <p>tension: <math>C_1 = 0.1</math></p> $n = \frac{N_0}{N_{pl,0}} + \frac{M_0}{M_{pl,0}}$

Table 3  
Axial force resistance for K joints CHS members to RHS chords (mode A). where  $N_{1,Rd}$  and  $N_{2,Rd}$  are the chord plasticisation failure load according to Eurocode 3 (2005) and Brazilian code;  $N_i^*$  is the chord plastification load according to CIDECT guide (Packer et al., 2009).

Joint	Braces			Chord			e (mm) (eccentricity)	g (mm) (gap)
	$d_i$ (mm)	$t_i$ (mm)	$\theta$ (mm)	$h_0$ (mm)	$b_0$ (mm)	$t$ (mm)		
K	48.3	3.7	47.7	60	110	4.8	23.50	32

Table 4  
Geometrical parameters of tested joints.

Braces		Chord	
$f_{y0}$ (MPa)	$f_{u0}$ (MPa)	$f_{y1,2}$ (MPa)	$f_{u1,2}$ (MPa)
456	555	250	325

Table 5  
Geometrical parameters of tested joints.

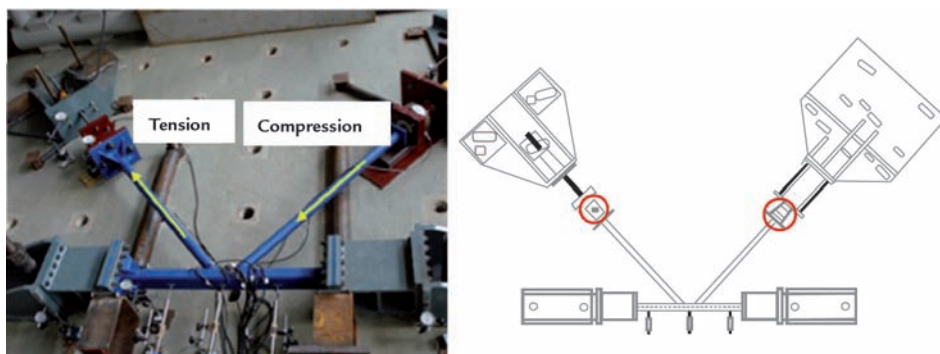


Figure 2  
General view of the test.

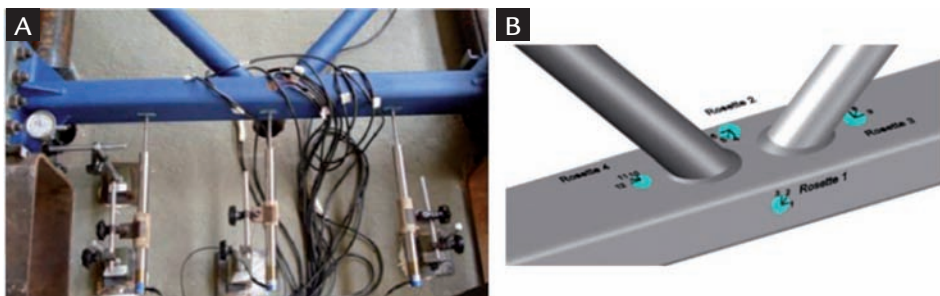


Figure 3  
View of the LVDT's and Rosettes' positions.

#### 4. Finite element analysis

The numerical model was developed by use of the finite element (ANSYS, 2007) with shell elements with four nodes. These elements had six degrees of freedom per node: translations  $x$ ,  $y$  and  $z$ , and rotations around  $x$ ,  $y$  and  $z$ . The analyses were performed taking into account their geometrical and physical non-linearity.

The welding was in accordance with previous studies that compared its influence on tubular joints and the element is the same used in the chord and brace modeling (SHELL 181). The

geometry of the numerical model took into account the curvature section, with twice the thickness of the chord (Mendes, Freitas and Freitas, 2012). The models use a material bilinear diagram based on the mechanical test of the steel used for the prototypes tested (Table 5). Figure 4 illustrates the mesh model used.

Ultimate joint resistance was determined using deformation limit criteria (Lu et al, 1994). This method considers the chord surface out of plane deformation occurring in failure

Mode A,  $\Delta$ , (Figure 5).

For joints that do not present defined load peaks, the ultimate load depends on the relationship between the ultimate load limit ( $N_{3\%}$ ) and the service limit ( $N_{1\%}$ ). If  $N_{3\%}/N_{1\%}$  is equal to or greater than 1.5, the service limit controls the resistance, which will be  $N_{1\%}$ . If  $N_{3\%}/N_{1\%}$  is less than 1.5, the ultimate limit controls the resistance, which will be  $N_{3\%}$ . Figure 6 illustrates this method for obtaining joint resistance, where  $N_{num}$  is defined as the resistance of the numerical model.

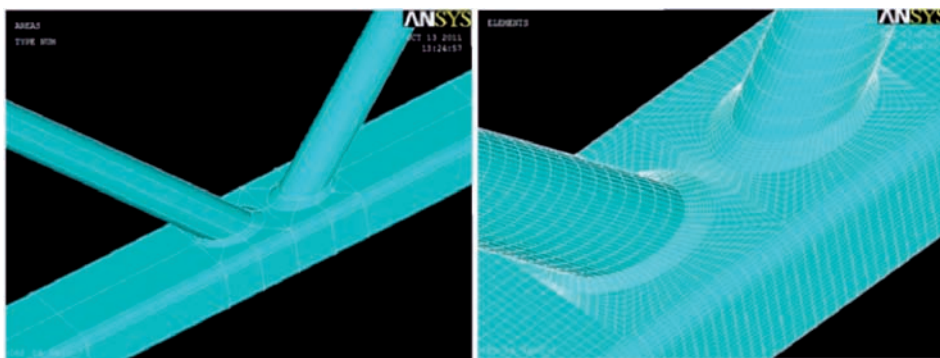


Figure 4  
The numerical mesh model for the joints.

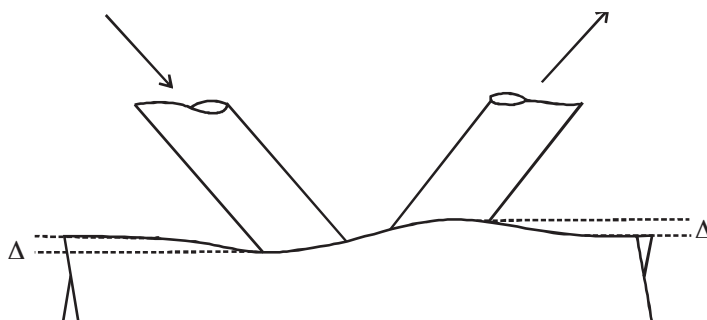


Figure 5  
Chord surface deformation,  $\Delta$ .

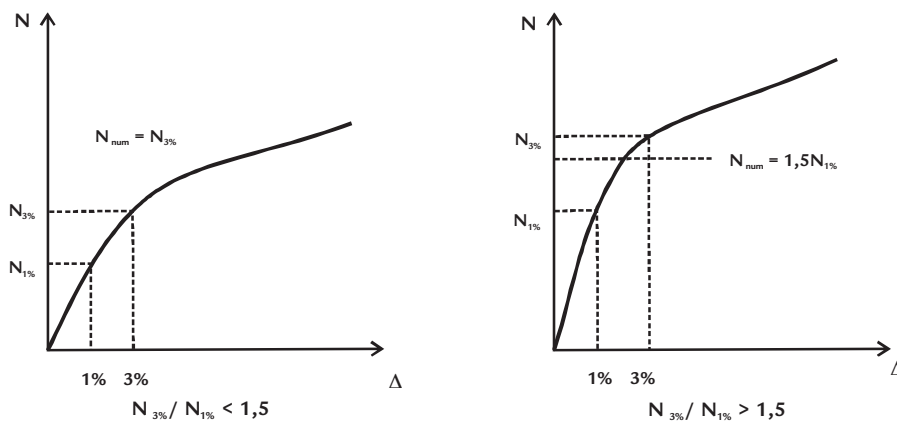


Figure 6  
Deformation limit criteria to ultimate load -  $N_{num}$  (Nunes, 2012).

### 5. Results

The Figure 7 shows the numerical model and the experimental results using von Mises deformation versus the brace under tension axial load for Tests K01 and K03. The results were compared using the rosette 2 data (Figure 3 B). Figure 7 shows a good agreement between the

numerical and experimental results (Nunes, 2012).

Table 7 presents the results of the developed parametrical analysis and the results for CHS to RHS K joints considering that Eurocode 3 (2005), Brazilian code and CIDECT formulations produce the same joint resistance

magnitudes. Analysing the results presented in Table 7, it can be concluded that when the parameter  $b$  increases, the joint resistance also increases. For some joints, the load magnitudes obtained with the numerical analysis were less than the ones evaluated with the adopted design codes.

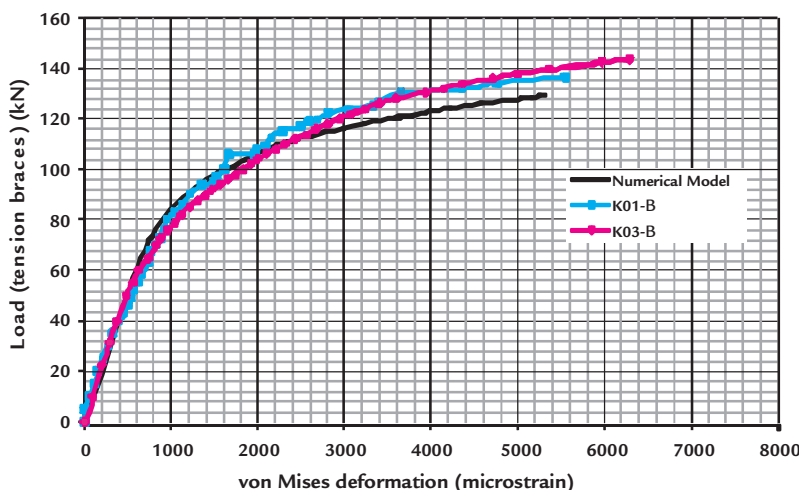


Figure 7  
von Mises deformation versus numerical and experimental loads – rosette 2.

$\beta$	$2\gamma$	$N_{i,Rd}$ (kN) (eurocode and PN)	$N_i$ (kN) (CIDECT)	$N_{1\%}$ (kN)	$N_{3\%}$ (kN)	$\frac{N_{3\%}}{N_{1\%}}$	$N_{num}$ (kN)	$\frac{N_{i,Rd}}{N_{Num}}$	$\frac{N_i}{N_{Num}}$
0.35	17.19	101.60	99.30	86	98	1.14	98	0.93	0.94
0.40		116.10	113.50	95	109	1.15	109	0.96	0.97
0.45		130.60	127.70	105	120	1.14	120	0.97	0.96
0.50		145.10	141.90	116.5	134	1.15	134	0.97	0.95
0.55		159.60	156.00	139	156	1.12	156	0.98	0.94
0.35	22.92	61.95	64.50	50	66	1.32	66	0.98	0.94
0.40		70.40	73.70	56	73	1.30	73	1.01	0.96
0.45		78.60	82.92	62	81	1.31	81	1.02	0.97
0.50		86.50	92.13	70	91	1.30	91	1.01	0.95
0.55		94.10	101.34	78	100	1.28	100	1.01	0.94
0.60	101.50	110.56	87	112	1.29	112	0.99	0.91	
0.35	28.0	71.78	77.35	56	77	1.38	77	1.00	0.93
0.40		81.70	88.40	61	85	1.39	85	1.04	0.96
0.45		91.50	99.45	67	94	1.40	94	1.06	0.97
0.50		101.10	110.50	73	102	1.40	102	1.08	0.99
0.55		110.40	121.55	81	112	1.38	112	1.09	0.99
0.60	119.30	132.60	91	124	1.36	124	1.07	0.96	

Table 7  
Theoretical and numerical resistance loads (Mode A).

$f_{y0}$  =250MPa (chord);  $f_{y1,2}$  =250MPa (braces);  $f_{u0}$  =325MPa (chord);  $f_{u1,2}$  =325MPa (braces).

## 6. Conclusion

The tested experimental models indicated the chord surface plasticity failure (Mode A). The instrumentation and test methodologies were efficient in evaluating the behavior and resistance of the joints. The numerical modeling of the welding, curvature, and shell elements, together with the

physical and geometrical non-linearity analyses, were efficient tools for joint evaluation. The numerical modeling results were in good agreement with the experimental model.

In relation to the failure mode, both the code regulations and the numerical modeling indicated Mode

A to be the one when experimentally observed. The resistance loads that were calculated according to Eurocode 3, Brazilian code and CIDECT have a good agreement with the numerical results, demonstrating the model's efficiency and thus, is indicated for use in other analyses.

## 7. Acknowledges

The authors gratefully acknowledge the Brazilian National and State Science

Support Agencies: CAPES, CNPq, FAPESP, FINEP, FINEP/MIG and to V&M DO BRASIL for the

financial support granted to this research program.

## 8. References

- ANSYS. *User's manual for revision 11*. Swanson Analysis Systems Inc. Houston, PA: 2007.
- Eurocode 3. *Design of steel structures - Structures - Part 1-8: General rules and rules for buildings*. Brussels: CEN, European Committee for Standardization, 2005. p.138.
- LU, L.H., WINKEL, G.D., YU, Y., WARDENIER, J. Deformation limit for the strength of hollow sections joints. In: INTERNATIONAL SYMPOSIUM ON TUBULAR STRUCTURES, 6. Melbourne, Australia, p. 341-347, 1994.
- MAYOR, I. S. *Análise teórico-experimental de ligações tipo K e KT compostas por perfis tubulares de seção retangular e circular*. Universidade Federal de Ouro Preto: 2010. (Dissertação de Mestrado in portuguese).
- NUNES, G. V. *Estudo paramétrico de ligações tipo "T", "K" e "KT" compostas por perfis tubulares de seção retangular e circular*. Universidade Federal de Ouro Preto: 2012. (Dissertação de mestrado in portuguese).
- MENDANHA, F. O., FREITAS, A. M. S., FREITAS, M. S. R., MUNIZ, C. D. G. Análise de ligações em perfis tubulares de aço do tipo K e KT com afastamento entre as diagonais e o montante. *REM - Revista Escola de Minas*, v. 60, n. 2, p.419-426, 2007.
- MENDES, F. C., FREITAS, M. S. R., FREITAS, A. M. S.. Estudo teórico experimental de ligações T e KT em perfis tubulares. *REM - Revista Escola de Minas*, v. 65, n.2, p. 175-180, 2012.
- PACKER, J.A., WARDENIER, J., ZHAO, X.-L., G.J. VAN DER VEGTE AND Y. KUROBANE, *Design Guide - For Rectangular Hollow Section (RHS) Joints Under Predominantly Static Loading*. (2nd Edition). Canadá: CIDECT, 2009. 149p.
- PN 02:125.03-004. *Projetos de estruturas de aço e de estruturas mistas de aço e concreto de edificações com perfis tubulares*. Rio de Janeiro: ABNT, 2011.
- WARDENIER, J., PACKER, J.A., ZHAO X-L AND VAN DER VEGTE, G.J. *Hollow Sections in Structural Applications*. Netherland: Bouwen met Staal, 2010. p.232.

---

Artigo recebido em 21 de agosto de 2012. Aprovado em 18 de março de 2013.